

# Visualization of 3 Distinct Retinal Plexuses by Projection-Resolved Optical Coherence Tomography Angiography in Diabetic Retinopathy

Thomas S. Hwang, MD; Miao Zhang, PhD; Kavita Bhavsar, MD; Xinbo Zhang, PhD; J. Peter Campbell, MD, MPH; Phoebe Lin, MD, PhD; Steven T. Bailey, MD; Christina J. Flaxel, MD; Andreas K. Lauer, MD; David J. Wilson, MD; David Huang, MD, PhD; Yali Jia, PhD

 Supplemental content

**IMPORTANCE** Projection artifacts in optical coherence tomography angiography (OCTA) blur the retinal vascular plexuses together and limit visualization of the individual plexuses.

**OBJECTIVE** To describe projection-resolved (PR) OCTA in eyes with diabetic retinopathy (DR) and healthy eyes.

**DESIGN, SETTING, AND PARTICIPANTS** In this case-control study, patients with DR and healthy controls were enrolled in this observational study from January 26, 2015, to December 4, 2015, at a tertiary academic center. Spectral-domain, 70-kHz OCT obtained 3 × 3-mm macular scans. The PR algorithm suppressed projection artifacts. A semiautomated segmentation algorithm divided PR-OCTA into superficial, intermediate, and deep retinal plexuses. Two masked graders examined 3-layer PR-OCTA and combined angiograms for nonperfusion and abnormal capillaries.

**MAIN OUTCOMES AND MEASURES** Retinal nonperfusion and capillary abnormalities and the diagnostic accuracy of detecting DR.

**RESULTS** Twenty-nine eyes of 15 healthy individuals (mean [SD] age, 36.2 [13.4] years; 11 women) and 47 eyes of 29 patients with DR (mean [SD] age, 55.5 [11.9]; 10 women) underwent imaging. PR-OCTA revealed 3 distinct retinal plexuses in their known anatomical locations in all eyes. The intermediate and deep plexuses of healthy eyes revealed capillary networks of uniform density and caliber, whereas the superficial plexus revealed vessels in the familiar centripetal branching pattern. In eyes with DR, 3-layer PR-OCTA disclosed incongruent areas of nonperfusion and varied vessel caliber and density in the deeper plexuses. Masked grading of capillary nonperfusion on 3-layer PR-OCTA detected DR with 100% sensitivity (95% CI, 90.8%-100%) and 100% specificity (95% CI, 85.4%-100%). With unsegmented retinal angiograms, the sensitivity and specificity were 78.7% (95% CI, 63.9%-88.8%) and 100% (95% CI, 85.4%-100%), respectively ( $P = .002$  for sensitivity). On 3-layer PR-OCTA, sensitivity was 72.2% (95% CI, 54.6%-85.2%) for severe nonproliferative DR and proliferative DR eyes with generalized nonperfusion in 2 or more individual plexuses, but on combined angiogram, sensitivity was 25.0% (95% CI, 12.7%-42.5%) for generalized nonperfusion ( $P < .001$ ). PR-OCTA disclosed dilated vessels in the intermediate and deep plexuses in 23 eyes (100%) with proliferative DR, 13 eyes (100%) with severe nonproliferative DR, 8 eyes (73%) with mild to moderate nonproliferative DR, and 0 control eyes.

**CONCLUSIONS AND RELEVANCE** By presenting 3 retinal vascular plexuses distinctly, PR-OCTA reveals capillary abnormalities in deeper layers with clarity and may distinguish DR from healthy eyes and severe DR from mild DR with greater accuracy compared with conventional OCTA.

*JAMA Ophthalmol.* doi:10.1001/jamaophthalmol.2016.4272  
Published online November 3, 2016.

**Author Affiliations:** Casey Eye Institute, Oregon Health & Science University, Portland.

**Corresponding Author:** Yali Jia, PhD, Casey Eye Institute, Oregon Health & Science University, 3375 SW Terwilliger Blvd, Portland, OR 97239 (jiaya@ohsu.edu).

The 3-dimensional (3-D) capabilities of optical coherence tomography angiography (OCTA) have reinvigorated interest in the retinal vascular layers.<sup>1,2</sup> Four distinct plexuses have previously been described.<sup>3</sup> Radial peripapillary capillaries are a distinct layer in the nerve fiber layer seen only near the optic disc. Three layers are present in the macula. The superficial capillary plexus is found in the ganglion cell layer. The intermediate plexus is concentrated between the inner plexiform layer (IPL) and the inner nuclear layer (INL) and the deep plexus between the INL and the outer plexiform layer (OPL). Entities such as paracentral acute middle maculopathy have further heightened interest in the intermediate and deep plexuses.<sup>4-6</sup>

Projection artifacts, however, pose a significant challenge in visualizing the 3 distinct retinal plexuses.<sup>7-9</sup> Moving red blood cells cast fluctuating shadows from superficial blood vessels to deeper layers,<sup>1,10,11</sup> and OCTA algorithms detect these shadows as motion. On cross-sectional angiograms, the projection artifacts appear as axial tails that blur the vascular layers together. On en face angiograms, these artifacts cause the superficial vasculature to appear to be superimposed onto deeper layers. Although terms such as *depth-resolved* angiography have been used,<sup>12</sup> projection artifacts have limited the ability of OCTA to truly resolve the depth of detected vessels.

To date, the approaches to deal with these artifacts have had significant tradeoffs. Slab subtraction, by replacing the cast of superficial vasculature with empty pixels in the en face angiograms of deeper layers, creates a negative artifact that disrupts vascular patterns.<sup>13,14</sup> Another approach is to displace the segmentation boundaries more posteriorly than the known anatomical borders to empirically diminish the strength of the projection signal. However, offsetting the boundaries brings into question the validity of observations made about the vascular layers.<sup>15</sup>

An approach was previously developed that resolves the ambiguity between true flow signal and projection artifacts.<sup>16</sup> The projection artifacts generally become weaker farther away from *in situ* flow but are dependent on the reflectance signal strength. The algorithm compares the flow signal normalized to the reflectance signal at the voxel to that of a more superficial voxel. If the signal is weaker than that of the superficial voxel, it is considered artifact and removed. If the signal is stronger, it is unlikely to be artifact and accepted as true flow. The resulting 3-D angiogram reveals the 3 plexuses in their true anatomical location as distinct vascular layers, which are demonstrated by distinct peaks of vessel density as a function of retinal depth with a few interconnecting vessels among the layers (Campbell et al, unpublished data, 2016).

In diabetic retinopathy (DR), the ability to observe individual capillary networks may enable earlier detection of microvasculopathy and a better understanding of the pathophysiological mechanisms.<sup>6,15,17</sup> We describe features of DR using this projection-resolved (PR)-OCTA and demonstrate the significance of investigating the 3 plexuses separately without projection artifacts.

## Key Points

**Question** Does projection-resolved optical coherence tomography angiography reveal more pathologic features in diabetic retinopathy?

**Findings** In this case-control study, projection-resolved optical coherence tomography angiography visualized 3 retinal plexuses distinctly and revealed nonperfusion and vascular abnormalities not evident on unsegmented retinal angiograms. Findings of 3-layer angiograms detected diabetic retinopathy more accurately compared with unsegmented retinal angiograms.

**Meaning** Although the clinical utility currently remains unknown, removing projection artifacts and visualizing the retinal plexuses in 3 layers may enhance the value of optical coherence tomography angiography in the evaluation of diabetic retinopathy.

## Methods

### Image Acquisition

A spectral-domain, 70-kHz OCT instrument (AngioVue, RTVue-XR; Optovue) obtained 3 × 3-mm macular scans for OCTA in healthy eyes and eyes with DR. Participants were recruited from the Casey Eye Institute with written informed consent under a protocol approved by the institutional review board of Oregon Health & Science University and in compliance with the Declaration of Helsinki.<sup>18</sup> All data were deidentified. Treating physicians obtained fluorescein angiography (FA) when clinically indicated. The severity of retinopathy was confirmed by an independent grader (K.B., J.P.C.) from standard Early Treatment Diabetic Retinopathy Study (ETDRS) 7-field photographs.<sup>19</sup> The eyes with significant media opacity or other significant macular pathologic features, such as vein occlusions, age-related macular degeneration, or significant idiopathic epiretinal membranes, were excluded.

Two B-scans, each consisting of 304 A-scans, were captured at each of 304 locations in 2.9 seconds. An x-fast scan and a y-fast scan were acquired, registered, and merged, minimizing motion artifacts. A commercial version of the split-spectrum amplitude-decorrelation angiography algorithm<sup>20</sup> detected blood flow.

### Image Processing

The projection-resolution algorithm<sup>16</sup> normalizes the detected flow signal by dividing the decorrelation value by the logarithm of reflectance intensity. The normalized signal is compared along each axial scan in the proximal to distal direction, identifying successive higher peaks as real vessels and removing smaller peaks. This method removes projection artifacts throughout the whole volume without referencing predefined slabs. The details of this algorithm and the demonstration of the separate vascular plexuses using this method were published in a separate work.<sup>16</sup>

A semiautomated algorithm then segmented this PR-OCTA into 3 slabs corresponding to the superficial, intermediate, and deep plexuses using structural OCT boundaries.<sup>21</sup> The superficial layer was defined as the inner 80% of ganglion cell

complex, which includes all structures between the internal limiting membrane (ILM) and the IPL-INL border. The intermediate layer was defined as the outer 20% of the ganglion cell complex and the inner 50% of the INL. The deep plexus was defined as the remaining slab internal to the outer boundaries of the OPL. This approach divides the INL into 2 halves that include the adjacent layers external and internal to the INL. The proportional method was chosen to deal with the foveal pit, where the inner retinal layers become very thin and the fixed thickness approach can force the segmentation into the outer retina, which should be normally avascular. In addition, this approach avoids meaningless segmentation of the capillaries at the foveal avascular zone (FAZ) edge, where the layers come together and the laminar structures taper and become discontinuous.<sup>22,23</sup>

Severe pathologic features sometimes caused the segmentation algorithm to fail and required manual correction. An advanced algorithm then automatically propagated the manual correction to the adjacent B-scans.<sup>21</sup>

### Grading of Images

Two masked graders (K.B., J.P.C.) examined the en face angiograms of each layer and the total inner retinal angiogram for capillary nonperfusion. The findings were localized using a modified ETDRS grid, dividing the  $3 \times 3$ -mm angiogram into a central 500- $\mu\text{m}$  circle and the remaining area into superior, inferior, nasal, and temporal quadrants. The grid was centered at the center of the image by default and adjusted by the grader to optimize the centration based on the vascular pattern. A modified grading scheme adapted from the ETDRS using 4 categories (no nonperfusion, questionable nonperfusion, definite focal nonperfusion, and definite generalized nonperfusion) was used to grade nonperfusion in each quadrant (eFigure 1 in the *Supplement*). To reduce confusion from the locally reduced signal that can simulate nonperfusion, the graders compared the angiograms to the en face reflectance maps. When there was a disagreement in grading, a third grader (T.S.H.) adjudicated the grading. The sensitivity and specificity of distinguishing DR from controls and severe DR from mild DR based on nonperfusion grading using the unsegmented vs segmented angiogram were analyzed. The McNemar test was used as the comparison and made with the same group of eyes.

The 2 masked graders also graded the intermediate and deep plexuses for the presence of focally dilated vessels and dilated vessels that form hairpin loops. The proportions of eyes with these findings in each DR severity group were compared.

## Results

### Patient Characteristics

Twenty-nine eyes from 15 healthy individuals (11 women; mean [SD] age, 36.2 [13.4] years; age range, 22-63 years) and 47 eyes from 29 patients with DR (10 women; mean [SD] age, 55.5 [11.9] years; range, 26-72 years) were imaged. Of the patients with DR, 13 (mean age, 49.1 years; 3 women) had proliferative diabetic retinopathy (PDR), 8 (mean age, 59.0 years; 1 woman) had

severe nonproliferative diabetic retinopathy (NPDR), and 8 (mean age, 60.0 years; 6 women) had mild to moderate NPDR. The patients were enrolled and underwent imaging from January 26, 2015, to December 4, 2015.

### Qualitative Description

PR-OCTA revealed 3 distinct vascular plexuses in the inner retina in healthy eyes (Figure 1) and eyes with DR (Figure 2 and Figure 3). In healthy eyes, the intermediate and deep plexuses were dense networks of capillaries of uniform density and caliber. In contrast, the superficial plexus contained both large and small vessels in a hierarchical branching pattern. Adjacent to the FAZ, the 3 plexuses merged into a single layer.

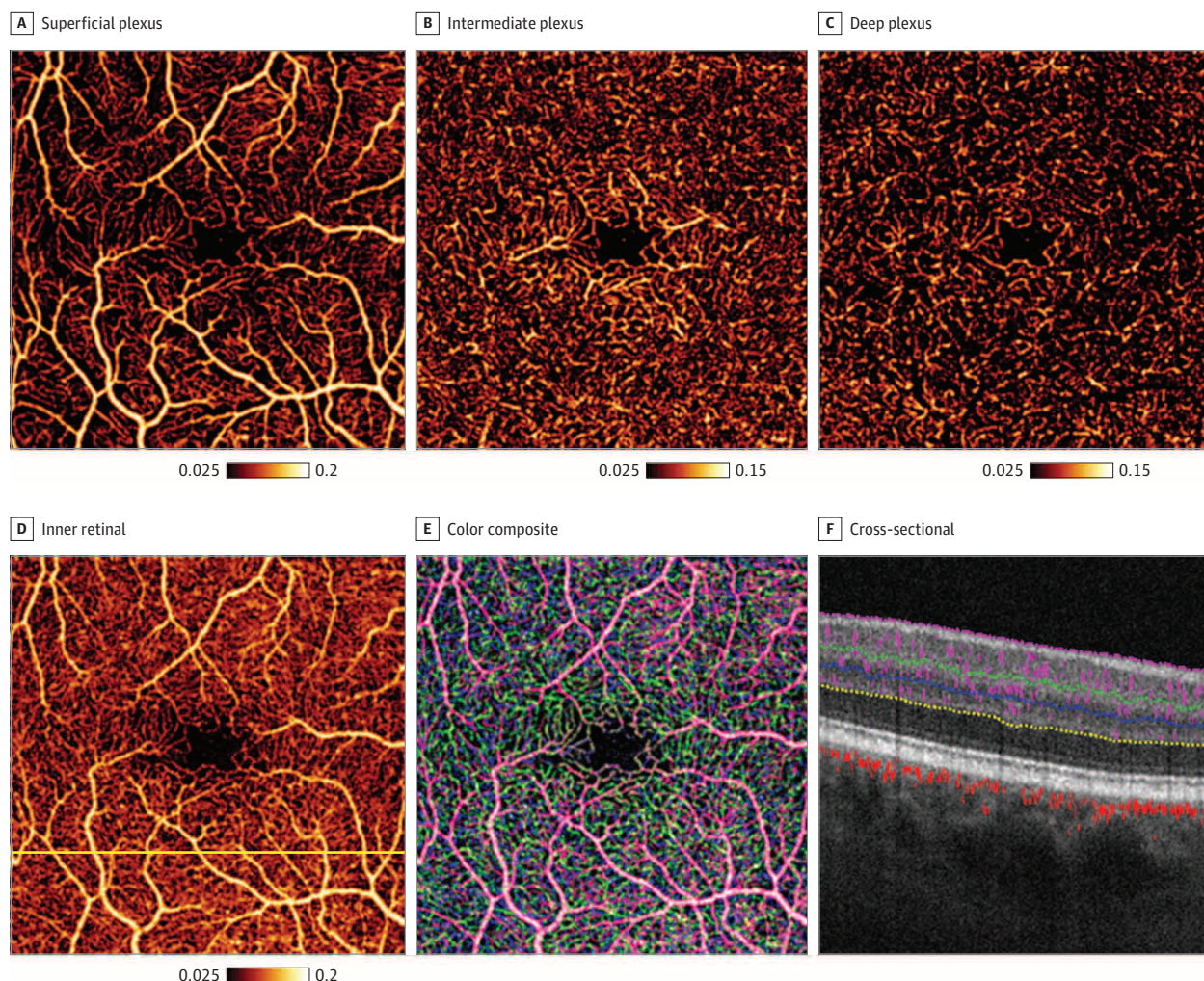
Figure 2 illustrates the difference in the 2-layer commercial retinal imaging output, 3-layer segmentation scheme without projection resolution, and PR-OCTA 3-layer segmentation. The retinal imaging system defines the superficial layer as 3  $\mu\text{m}$  below the ILM to 15  $\mu\text{m}$  below the IPL, which includes most of the superficial and intermediate plexuses defined in 3-layer segmentation. As a result, an area of nonperfusion seen on superficial plexus of the 3-layer scheme was obscured in the retinal imaging output, apparently by vessels that the intermediate plexus included in the superficial slab. As expected, the superficial plexuses in the 3-layer segmentation with and without projection resolution were similar. However, the intermediate plexus without projection resolution had a strong artifact from the superficial plexus, obscuring the unique vascular patterns seen in the PR-OCTA version. The retinal imaging system defines the deep slab as 15 to 70  $\mu\text{m}$  below the IPL, which reveals an image similar to the deep plexus in the 3-layer scheme without projection resolution. Although not as obviously imprinted with superficial vasculature as the intermediate plexus, projection artifacts were evident. Larger superficial vessels projected to this layer as linear vessels, and smaller superficial vessels gave an impression of higher vessel density compared with the PR-OCTA deep plexus image.

PR-OCTA revealed incongruent areas of nonperfusion in the 3 plexuses in DR eyes, revealing areas not evident when the entire retinal circulation was projected in an undifferentiated inner retinal slab or FA. Microaneurysms appeared to cross the slab boundaries (Figure 2). The intermediate and deep plexuses, in addition to showing areas of nonperfusion, revealed varied vessel diameter in eyes with DR (Figures 2 and 3). In some eyes, prominent, dilated linear vessels in the deeper plexuses, frequently associated with nonperfusion, were visible on FA (Figure 2). In several eyes with PDR, discrete, small hairpin loops of dilated vessels that traverse into the adjacent slab without violating the ILM were present in areas of nonperfusion (Figure 3). These vessels were sometimes faintly visible on FA. In one eye, a network of dilated vessels in the deeper layers connected to a frond of retinal neovascularization near the fovea (eFigure 2 in the *Supplement*).

### Grading of Angiograms

In eyes with DR, a combined inner retinal angiogram revealed definite nonperfusion with a sensitivity of 78.7% (37 of 47 patients) (95% CI, 63.9%-88.8%), whereas the segmented

Figure 1. En Face 3 × 3-mm Projection-Resolved Optical Coherence Tomography Angiogram of a Healthy Eye



Three vascular plexuses with distinct vascular patterns are shown (A-C). Combined inner retinal (D) (yellow line marks the position of the cross-sectional angiogram) and color composite (E) (purple indicates superficial plexus; green, intermediate plexus; and blue, deep plexus) angiograms show the plexuses

together. A cross-sectional angiogram (F) shows the segmentation scheme (white indicates optical coherence tomography; purple, inner retinal blood flow; and red, choroidal blood flow).

PR-OCTA revealed definite nonperfusion in at least one of the plexuses in all eyes with DR. None of the control eyes had definite nonperfusion in combined or segmented angiograms (Table 1). In general, more quadrants with nonperfusion were present in eyes with more severe DR in segmented or combined angiograms. The presence of nonperfusion in the 3-layer PR-OCTA distinguished eyes with DR from control eyes with greater sensitivity than with combined inner retinal angiogram ( $P = .002$ , McNemar test) (Table 2). With the use of generalized nonperfusion within a subfield as a criterion, grading using 3-layer PR-OCTA also distinguished severe DR from mild DR with greater sensitivity ( $P < .001$ , McNemar test) compared with combined retinal angiogram (Table 2).

All eyes with PDR or severe NPDR had dilated vessels in intermediate and deep plexuses. Eight of 11 eyes (73%) with mild to moderate NPDR had dilated vessels in those plexuses. None of the control eyes had dilated vessels in the

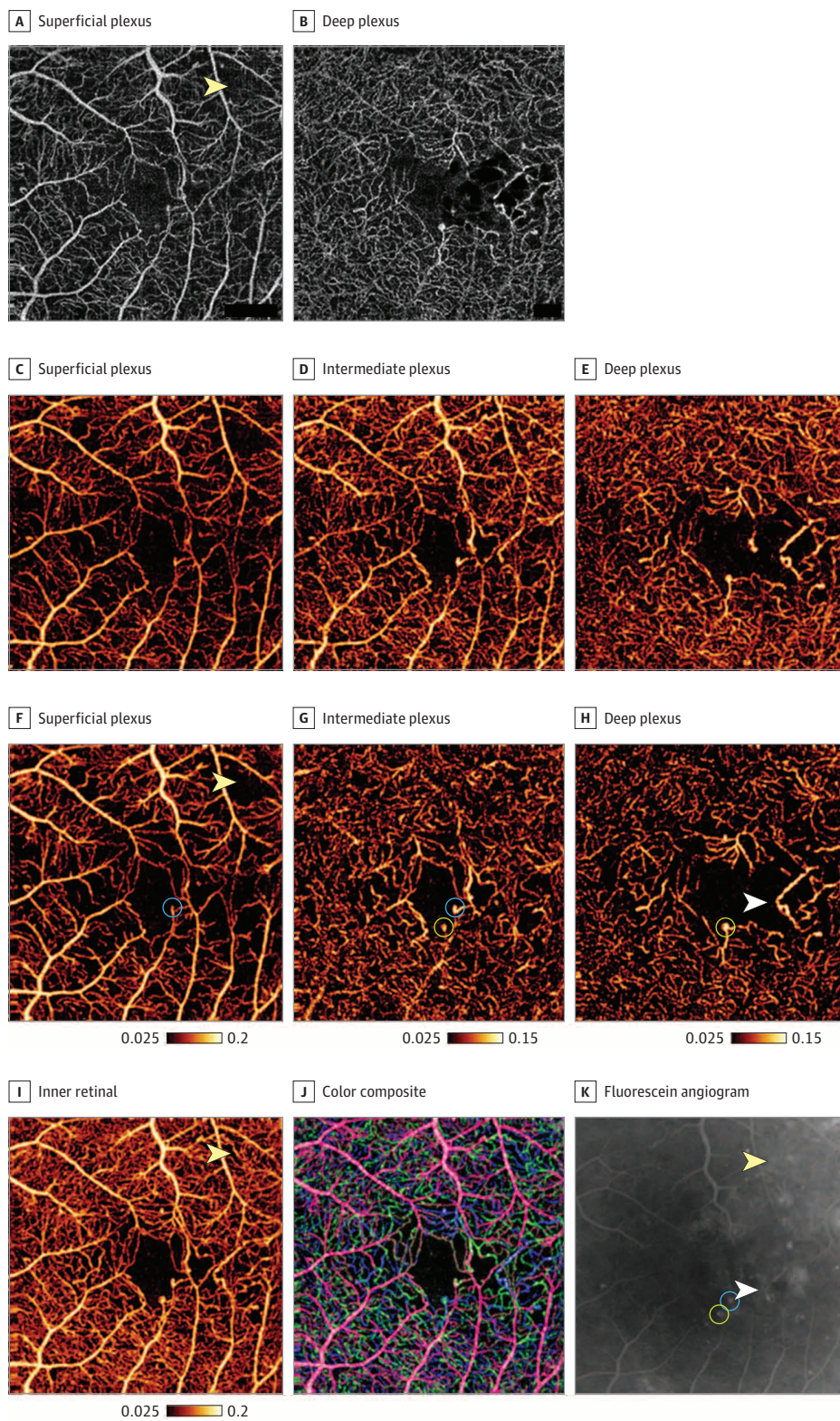
deeper plexuses. Nine of 23 eyes with PDR (39%) had dilated vessels that formed hairpin loops. None of the eyes with NPDR or no retinopathy had these hairpin loops (eTable in the Supplement).

The interobserver reliability between the 2 masked graders was assessed with the Cohen  $\kappa$ . On nonperfusion grading,  $\kappa$  was 0.75 and 0.80 for within 1-step agreement for combined inner retina and 3-layer segmented angiograms, respectively. For the grading of dilated vessels in 3-layer segmented angiograms, the  $\kappa$  was 0.88.

## Discussion

In this work, we describe the features of DR visualized using a technique that resolves the ambiguity between the decorrelation signal from projection artifacts and *in situ* flow

**Figure 2.** En Face  $3 \times 3\text{-mm}$  Optical Coherence Tomography Angiogram (OCTA) of Nonproliferative Diabetic Retinopathy

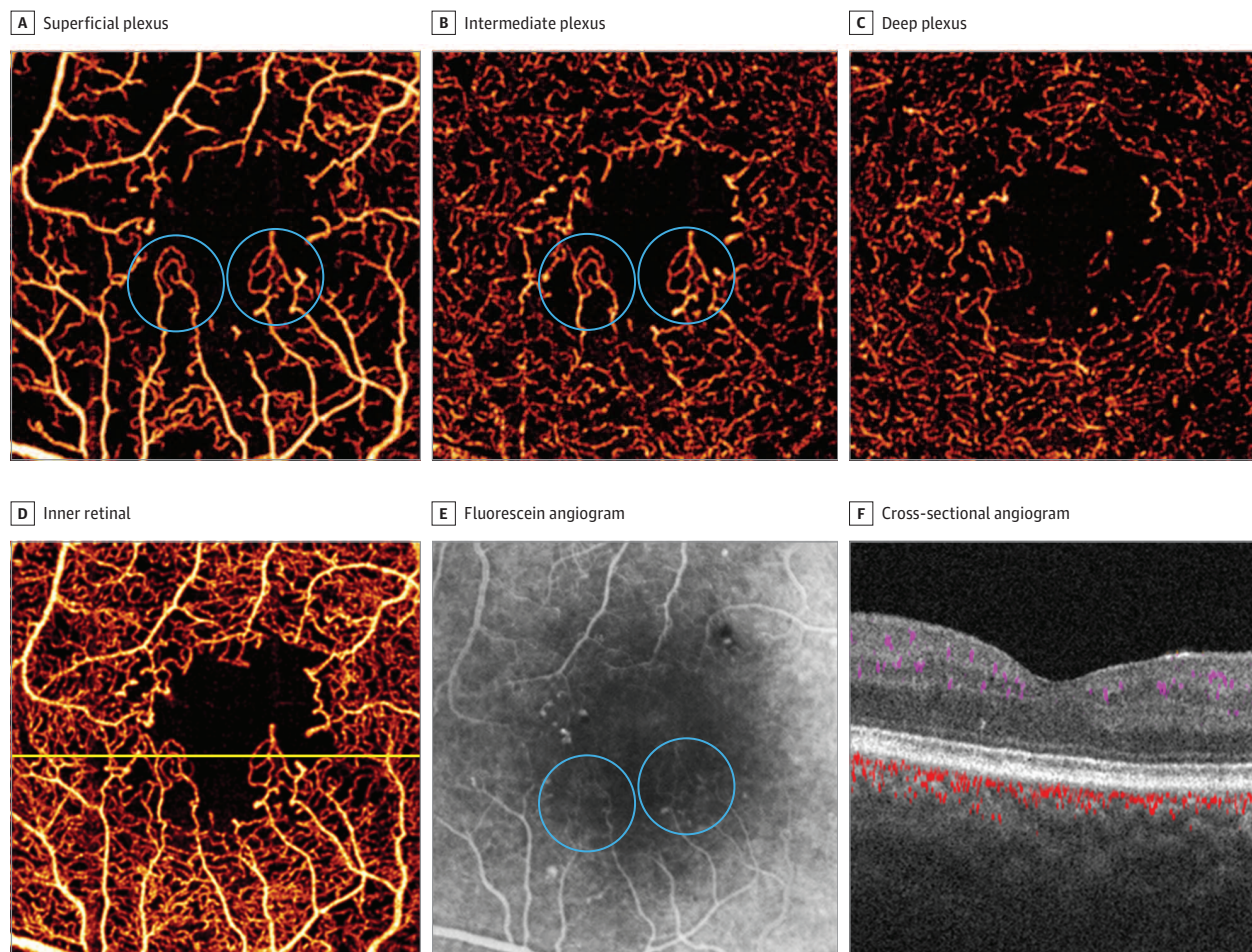


Difference in the 2-layer commercial imaging system output (A and B), 3-layer segmentation scheme without projection resolution (C-E), and projection-resolved OCTA 3-layer segmentation (F-H). Yellow arrowheads indicate a nonperfusion area in the superficial plexus, which cannot be seen in the combined inner retinal angiogram (I) or fluorescein angiogram (K); white arrowheads, dilated vessels; and blue and yellow circles, 2 microaneurysms. In the color composite (J), purple indicates superficial plexus; green, intermediate plexus; and blue, deep plexus.

throughout the 3-D angiogram.<sup>16</sup> The PR-OCTA technique combined with advanced semiautomated segmentation software<sup>21</sup>

allowed segmentation of the retinal vasculature into 3 distinct vascular plexuses along the known anatomical bound-

**Figure 3. Extensive Capillary Nonperfusion in the Superficial Plexus Not Evident on an Unsegmented Retinal Optical Coherence Tomography Angiogram or a Fluorescein Angiogram (FA)**



Superficial (A), intermediate (B), and deep (C) plexuses. A combined inner retinal angiogram (D) (yellow line marks the position of the cross-sectional angiogram) shows the plexuses together. An FA (E) shows loops of dilated vessels in areas of nonperfusion. A cross-sectional angiogram (F) shows the

segmentation scheme. Blue circles indicate loops of dilated vessels in areas of nonperfusion in the superficial and intermediate plexuses and the FA. The intermediate and deep plexuses have patchy areas of nonperfusion with irregular vessel caliber and a few dilated vessels.

aries and visualized distinct patterns of nonperfusion and vascular anomalies in eyes with DR not seen with combined inner retinal angiograms.

In a recent work on volume-rendered OCTA, Spaide,<sup>24</sup> citing the loss of laminar structures in DR that can make segmentation difficult, advocated for an approach that visualizes the deeper layers by using the scleral perspective and avoids segmentation altogether. In this study, we found that a semiautomated segmentation algorithm can separate the retinal vasculature into 3 distinct plexuses in eyes with a full spectrum of DR severity. Manual correction was required in half of the diabetic eyes with significant pathologic features, which then could be propagated to adjacent frames automatically.<sup>21</sup> Furthermore, the use of the scleral perspective to visualize the deeper layers is not immune to projection artifacts because the tail of the projection artifact from the superficial vessels can extend posteriorly past the intermediate and deep plexuses.<sup>16,25</sup> Viewed from the posterior

vantage point, the superficial vasculature can appear in front of the deep vessels because of projection artifacts and obscure the deep vessels. Even if projection artifacts were not an issue, the intermediate vascular plexus could not be visualized with this approach.

Some authors have considered the retinal vasculature to consist of 2 layers: superficial and deep, with the latter including both layers flanking the INL (considered intermediate and deep plexuses in this work).<sup>2,25,26</sup> The current commercial OCTA systems have generally adopted this understanding. However, the typical reported segmentation scheme for the superficial layer starts a little posterior to the ILM and 15 µm posterior to the IPL. This scheme includes nearly 50% of the area anterior to the INL, where we expect to see the intermediate plexus or half of the deep plexus in the prevalent 2 layers. This posterior offsetting of the segmentation boundaries posteriorly can reduce the projection artifacts seen on en face images.<sup>10,11</sup> However, inclusion of the intermediate plexus into

**Table 1. Comparison of Nonperfusion Grading Between Combined vs 3-Layer Separated Angiograms**

Angiogram	PDR (n = 23)	Severe NPDR (n = 13)	Mild to Moderate NPDR (n = 11)	Control (n = 29)
Combined inner retina				
No definite nonperfusion <sup>a</sup>	4	4	2	29
≥1 Quadrant with definite or generalized nonperfusion	19	9	9	0
≥1 Quadrant with generalized nonperfusion	4	5	1	0
Mean No. of quadrants with definite or generalized nonperfusion	2.78	2.15	1.82	0
Segmented superficial/intermediate/deep angiograms				
No definite nonperfusion <sup>a</sup>	1/2/0	0/0/0	0/4/3	29/29/29
≥1 Quadrant with definite or generalized nonperfusion	22/21/23	13/13/13	11/7/8	0/0/0
≥1 Quadrant with generalized nonperfusion	18/8/17	9/8/12	2/1/5	0/0/0
Mean No. of quadrants with definite or generalized nonperfusion	3.7/3.4/3.9	4/3.9/4	3.7/1.9/2.8	0/0/0
≥2 Layers with generalized nonperfusion	15	11	2	0

Abbreviations: NPDR, nonproliferative diabetic retinopathy; PDR, proliferative diabetic retinopathy.

<sup>a</sup> No definite nonperfusion includes no nonperfusion and questionable nonperfusion grading.

**Table 2. Diagnostic Accuracy of Projection-Resolved OCTA Features in DR**

Feature	No. of Patients	Sensitivity (95% CI)	Specificity (95% CI)
En face OCTA of combined inner retina circulation (≥1 quadrant with definite nonperfusion/no definite nonperfusion <sup>a</sup> )			
DR	37/10		
No DR	0/29	78.7 (63.9-88.8)	100 (85.4-100)
En face OCTA of 3 separate retinal plexuses (≥1 quadrant with definite nonperfusion/no definite nonperfusion <sup>a</sup> )			
DR	48/0		
No DR	0/29	100 (90.8-100)	100 (85.4-100)
En face OCTA of combined inner retinal circulation (total inner retina in any quadrant with generalized nonperfusion/total inner retina with no generalized nonperfusion)			
Severe DR <sup>b</sup>	9/27		
Mild DR <sup>c</sup>	1/10	25.0 (12.7-42.5)	90.9 (57.1-99.5)
En face OCTA of 3 separate retinal plexuses (2 or 3 plexuses with ≥1 quadrant of generalized nonperfusion/0 or 1 plexus with any generalized nonperfusion)			
Severe DR <sup>b</sup>	26/10		
Mild DR <sup>c</sup>	2/9	72.2 (54.6-85.2)	81.8 (47.8-96.8)

Abbreviations: DR, diabetic retinopathy; NPDR, nonproliferative diabetic retinopathy; OCTA, optical coherence tomography angiography; PDR, proliferative diabetic retinopathy.

<sup>a</sup> No definite nonperfusion includes no nonperfusion and questionable nonperfusion grading.

<sup>b</sup> Severe DR includes PDR and severe NPDR.

<sup>c</sup> Mild DR includes mild to moderate NPDR.

the superficial slab adds to the uncertainty about the validity of observations made with this segmentation scheme.

Park et al<sup>15</sup> recently described en face visualization of the intermediate capillary plexus by manually segmenting the 3-D angiogram. However, the best results were achieved by segmenting external to known anatomical boundaries to minimize projection artifacts. This method reduced but did not eliminate projection artifacts, especially in the intermediate plexus, making it difficult to objectively distinguish true capillaries of a slab vs projected capillaries. In addition, the segmentation scheme defined the intermediate plexus to capture the entire INL and the deep plexus to be in the OPL. This means that the intermediate slab in this scheme very likely includes the deep plexus vessels, and the deep slab may not include all the vessels of the deep plexuses.

Examination of the individual plexuses using the PR technique increased the sensitivity of detecting DR and severe DR compared with the combined inner retinal angiogram in this qualitative study. In this limited patient set, the nonperfusion area on the 3 × 3-mm segmented angiograms detected DR with 100% sensitivity and specificity. Although we used masked, trained retina specialists for the grading, qualitative grading of nonperfusion in angiography has known limitations in objectivity and interobserver reliability.<sup>19</sup> Automated detection and quantification of capillary nonperfusion<sup>17</sup> with the segmented angiograms may make this a more objective and practical tool in the management of DR.

A novel type of vascular abnormality that can be identified in PR-OCTA is dilated vessels in the deeper plexuses that sometimes form hairpin loops in areas of nonperfusion. These

lesions are consistent with intraretinal neovascularization (IRNV), as reported by Muraoka and Shimizu.<sup>27</sup> They followed up patients with diabetic eyes with FA for return of blood flow in nonperfused areas. In a few eyes, they observed return of flow to normal capillaries. For most eyes, they observed dilated vessels in previously ischemic areas with minimal dye leakage and a tendency to form hairpin loops, which they termed IRNV. These lesions are likely related to the clinical findings of intraretinal microvascular abnormality. Although IRNV has been described histologically, reports of these lesions are sparse in the literature despite their potential for being a marker for preproliferative disease.<sup>28</sup> This finding is possibly attributable to the difficulty in identifying these lesions with conventional imaging. With PR-OCTA, dilated vessels in the deeper plexuses, some of which form hairpin loops, are seen easily. These dilated vessels were highly correlated with severe DR in this study. The hairpin configuration of the dilated vessels was found only in eyes with PDR, further supporting the theory that these lesions are indeed IRNV. Further study is necessary to evaluate the role of these findings in the management of DR.

We did not grade the FAZ size or contour using the 3-layer segmentation in this study. In healthy eyes, the 3 vascular plexuses merge at the edge of the FAZ as the laminar structures used for segmentation thin at the foveal pit. As a result, the segmentation scheme can change the size and shape of the FAZ. For example, a scheme that uses a fixed slab thickness and the IPL as the inner limit can force the slab to dip into avascular outer retina, resulting in a FAZ that is purely a function of the foveal pit contour. Although a clear association between the

foveal pit shape and the FAZ size exists,<sup>29</sup> this association in retinal vascular disease may be complex. With current technology, we do not think one could form conclusions about which plexus a capillary belongs to as it approaches the FAZ edge in the foveal pit.

### Limitations

Limitations of this study include its qualitative and cross-sectional design, modest number of participants, and a non-age-matched control group. An association between OCTA vessel density and age has been reported for healthy eyes,<sup>30</sup> and it is possible that having a younger control group could alter the diagnostic accuracy estimated by this study. However, it is not known whether these OCTA features that are visible to human observers would be age dependent, especially when the differences in vessel density between older and younger patients, although statistically significant, were small. A larger patient cohort with prospective follow-up and age-matched controls may yield clearer insights about the vascular lesions described in this study.

### Conclusions

PR-OCTA reveals the 3 retinal vascular plexuses distinctly in their true anatomical location and visualizes pathologic features not previously seen on conventional OCTA. Application of this technology in DR may yield new understanding about the disease and make OCTA more useful for qualitative and quantitative analysis.

#### ARTICLE INFORMATION

**Accepted for Publication:** September 18, 2016.

**Published Online:** November 3, 2016.

**doi:**10.1001/jamaophthalmol.2016.4272

**Author Contributions:** Dr Jia had full access to all the data in the study and takes responsibility for the integrity of the data and the accuracy of the data analysis.

*Study concept and design:* Hwang, Huang, Jia.

*Acquisition, analysis, or interpretation of data:*

Hwang, M. Zhang, Bhavsar, X. Zhang, Campbell, Lin, Bailey, Flaxel, Lauer, Wilson, Huang.

*Drafting of the manuscript:* Hwang, M. Zhang.

*Critical revision of the manuscript for important intellectual content:* All authors.

*Statistical analysis:* Hwang, X. Zhang.

*Obtained funding:* Wilson, Jia.

*Administrative, technical, or material support:*

Hwang, M. Zhang, Bhavsar, Campbell, Bailey, Lauer, Wilson, Huang.

**Conflict of Interest Disclosures:** All authors have completed and submitted the ICMJE Form for Disclosure of Potential Conflicts of Interest. Drs Jia and Huang reported having a significant financial interest in Optovue Inc, a company that may have a commercial interest in the results of this research and technology. Dr Huang also has a financial interest in Carl Zeiss Meditec Inc. Dr Lauer consults for Oxford Biomedica. No other disclosures were reported.

**Funding/Support:** This work was supported by grants DP3 DK104397 (Drs Jia and Wilson),

RO1 EY024544 (Dr Jia), RO1 EY023285 (Dr Huang), and P30 EY010572 from the National Institutes of Health and by unrestricted departmental funding from Research to Prevent Blindness.

**Role of the Funder/Sponsor:** The funding sources had no role in the design and conduct of the study; collection, management, analysis, and interpretation of the data; preparation, review, or approval of the manuscript; and the decision to submit the manuscript for publication.

#### REFERENCES

- Jia Y, Bailey ST, Hwang TS, et al. Quantitative optical coherence tomography angiography of vascular abnormalities in the living human eye. *Proc Natl Acad Sci U S A*. 2015;112(18):E2395-E2402.
- Spaide RF, Klancnik JM Jr, Cooney MJ. Retinal vascular layers imaged by fluorescein angiography and optical coherence tomography angiography. *JAMA Ophthalmol*. 2015;133(1):45-50.
- Chan G, Balaratnasingam C, Yu PK, et al. Quantitative morphometry of perifoveal capillary networks in the human retina. *Invest Ophthalmol Vis Sci*. 2012;53(9):5502-5514.
- Rahimy E, Sarraf D, Dollin ML, Pitcher JD, Ho AC. Paracentral acute middle maculopathy in nonischemic central retinal vein occlusion. *Am J Ophthalmol*. 2014;158(2):372-380.e1.
- Nemiroff J, Kuehlewein L, Rahimy E, et al. Assessing deep retinal capillary ischemia in paracentral acute middle maculopathy by optical coherence tomography angiography. *Am J Ophthalmol*. 2016;162(2):121-132.e1.
- Chen X, Rahimy E, Sergott RC, et al. Spectrum of retinal vascular diseases associated with paracentral acute middle maculopathy. *Am J Ophthalmol*. 2015;160(1):26-34.e1.
- Hwang TS, Jia Y, Gao SS, et al. Optical coherence tomography angiography features of diabetic retinopathy. *Retina*. 2015;35(11):2371-2376.
- Ishibazawa A, Nagaoka T, Takahashi A, et al. Optical coherence tomography angiography in diabetic retinopathy: a prospective pilot study. *Am J Ophthalmol*. 2015;160(1):35-44.e1.
- Cole ED, Novais EA, Louzada RN, Waheed NK. Contemporary retinal imaging techniques in diabetic retinopathy: a review. *Clin Exp Ophthalmol*. 2016;44(4):289-299.
- Huang D, Jia Y, Gao SS. Principles of optical coherence tomography angiography. In: Lumbros BHD, Rosenfield P, Chen C, Rispoli M, Romano A, eds. *OCT Angiography Atlas*. New Delhi, India: Jaypee Brothers Medical Publishers; 2015:3-7.
- Huang D, Jia Y, Gao SS. Interpretation of optical coherence tomography angiography. In: Lumbros BHD, Rosenfield P, Chen C, Rispoli M, Romano A, eds. *OCT Angiography Atlas*. New Delhi, India: Jaypee Brothers Medical Publishers; 2015:8-14.
- An L, Shen TT, Wang RK. Using ultrahigh sensitive optical microangiography to achieve comprehensive depth resolved microvasculature

- mapping for human retina. *J Biomed Opt.* 2011;16(10):106013-106019.
- 13.** Liu L, Gao SS, Bailey ST, Huang D, Li D, Jia Y. Automated choroidal neovascularization detection algorithm for optical coherence tomography angiography. *Biomed Opt Express.* 2015;6(9):3564-3576.
- 14.** Zhang A, Zhang Q, Wang RK. Minimizing projection artifacts for accurate presentation of choroidal neovascularization in OCT micro-angiography. *Biomed Opt Express.* 2015;6(10):4130-4143.
- 15.** Park JJ, Soetikno BT, Fawzi AA. Characterization of the middle capillary plexus using optical coherence tomography angiography in healthy and diabetic eyes [published online May 19, 2016]. *Retina.* doi:10.1097/IAE.00000000000001077
- 16.** Zhang M, Hwang TS, Campbell JP, et al. Projection-resolved optical coherence tomographic angiography. *Biomed Opt Express.* 2016;7(3):816-828.
- 17.** Hwang TS, Gao SS, Liu L, et al. Automated quantification of capillary nonperfusion using optical coherence tomography angiography in diabetic retinopathy. *JAMA Ophthalmol.* 2016;134(4):367-373.
- 18.** World Medical Association. World Medical Association Declaration of Helsinki: ethical principles for medical research involving human subjects. *JAMA.* 2013;310(20):2191-2194. doi:10.1001/jama.2013.281053
- 19.** Early Treatment Diabetic Retinopathy Study Research Group. Classification of diabetic retinopathy from fluorescein angiograms: ETDRS report number 11. *Ophthalmology.* 1991;98(5)(suppl):807-822.
- 20.** Jia Y, Tan O, Tokayer J, et al. Split-spectrum amplitude-decorrelation angiography with optical coherence tomography. *Opt Express.* 2012;20(4):4710-4725.
- 21.** Zhang M, Wang J, Pechauer AD, et al. Advanced image processing for optical coherence tomographic angiography of macular diseases. *Biomed Opt Express.* 2015;6(12):4661-4675.
- 22.** Snodderly DM, Weinhaus RS, Choi JC. Neural-vascular relationships in central retina of macaque monkeys (*Macaca fascicularis*). *J Neurosci.* 1992;12(4):1169-1193.
- 23.** Snodderly DM, Weinhaus RS. Retinal vasculature of the fovea of the squirrel monkey, *Saimiri sciureus*: three-dimensional architecture, visual screening, and relationships to the neuronal layers. *J Comp Neurol.* 1990;297(1):145-163.
- 24.** Spaide RF. Volume-rendered optical coherence tomography of diabetic retinopathy pilot study. *Am J Ophthalmol.* 2015;160(6):1200-1210.
- 25.** Bonnin S, Mané V, Couturier A, et al. New insight into the macular deep vascular plexus imaged by optical coherence tomography angiography. *Retina.* 2015;35(11):2347-2352.
- 26.** Savastano MC, Lumbroso B, Rispoli M. In vivo characterization of retinal vascularization morphology using optical coherence tomography angiography. *Retina.* 2015;35(11):2196-2203.
- 27.** Muraoka K, Shimizu K. Intraretinal neovascularization in diabetic retinopathy. *Ophthalmology.* 1984;91(12):1440-1446.
- 28.** Proia AD, Caldwell MC. Intraretinal neovascularization in diabetic retinopathy. *Arch Ophthalmol.* 2010;128(1):142-144.
- 29.** Dubis AM, Hansen BR, Cooper RF, Beringer J, Dubra A, Carroll J. Relationship between the foveal avascular zone and foveal pit morphology. *Invest Ophthalmol Vis Sci.* 2012;53(3):1628-1636.
- 30.** Coscas F, Sellam A, Glacet-Bernard A, et al. Normative data for vascular density in superficial and deep capillary plexuses of healthy adults assessed by optical coherence tomography angiography. *Invest Ophthalmol Vis Sci.* 2016;57(9):OCT21-OCT223.

## **Supplementary Online Content**

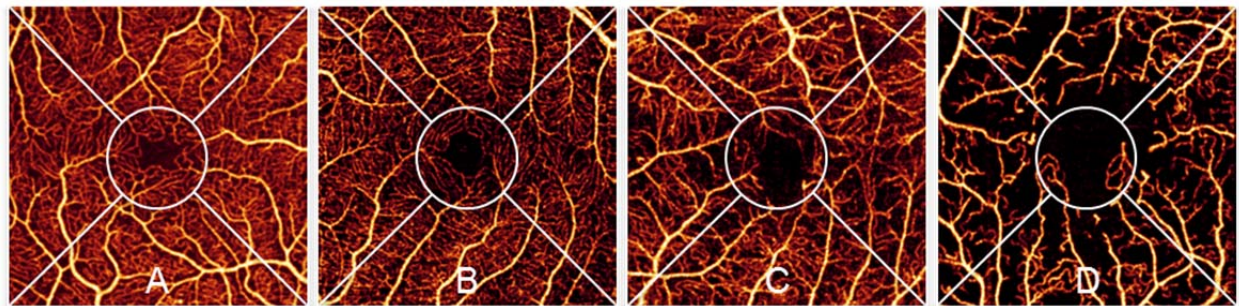
Hwang TS, Zhang M, Bhavsar K, et al. Visualization of 3 distinct retinal plexuses by projection-resolved optical coherence tomography angiography in diabetic retinopathy. *JAMA Ophthalmol*. Published online November 3, 2016.  
doi:10.1001/jamaophthalmol.2016.4272

**eFigure 1.** Representative 3 × 3-mm Segmented Inner Plexus Angiograms

**eFigure 2.** An Eye With Parafoveal Neovascularization

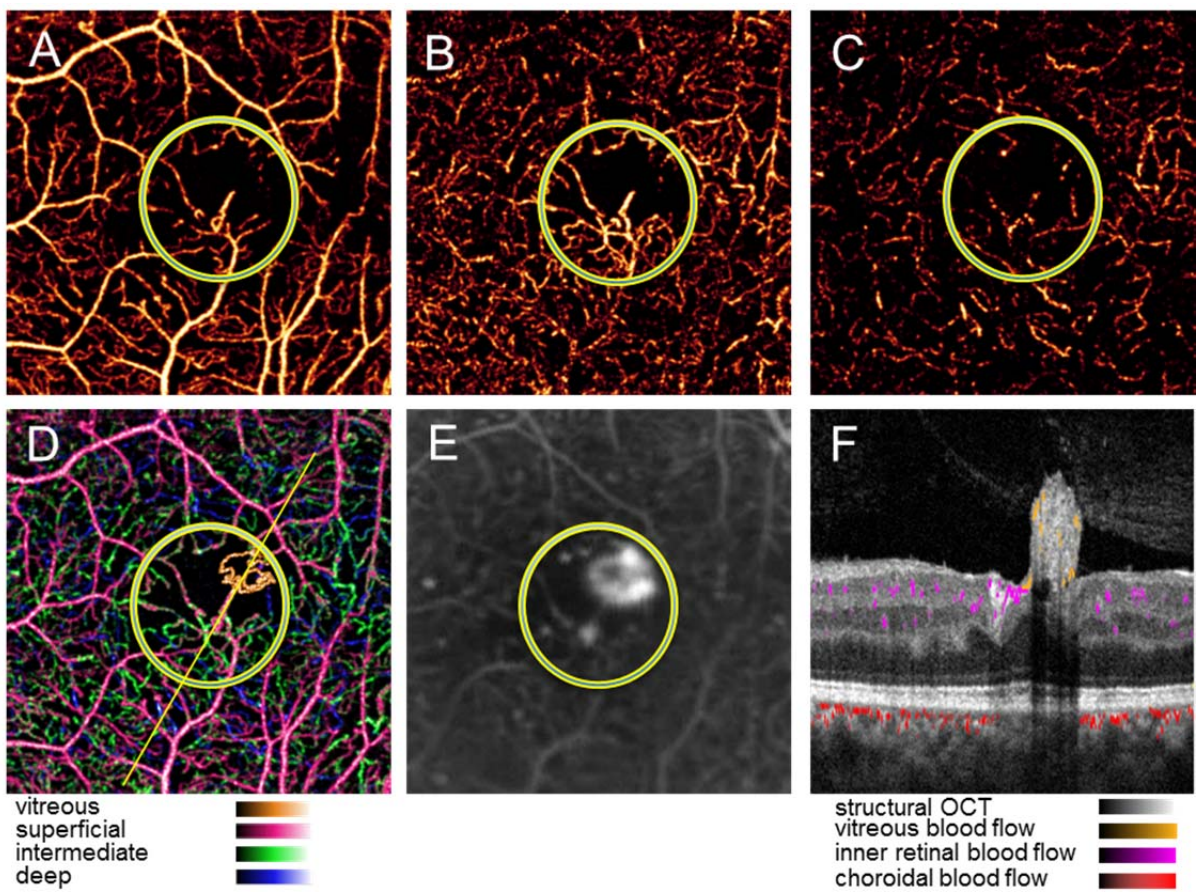
**eTable.** Dilated Vessels in Intermediate and Deep Plexuses

This supplementary material has been provided by the authors to give readers additional information about their work.



**eFigure 1.** Representative  $3 \times 3$ -mm Segmented Inner Plexus Angiograms

Representative 3x3mm segmented inner plexus angiograms with (A) no nonperfusion, (B) questionable nonperfusion, with areas of lower signal either in low reflectance area (superior quadrant adjacent to the central circle) or motion artifact (subtle vertical line at the right edge), (C) definite focal nonperfusion, and (D) definite generalized nonperfusion. Each angiogram is divided into central circle with 1mm diameter and the remainder divided into superior, inferior, nasal and temporal quadrants. Similar evaluation was done for the intermediate and deep plexuses.



**eFigure 2.** An Eye With Parafoveal Neovascularization

An eye with parafoveal neovascularization (NV) shown in orange within the yellow circle in composite angiogram (D) and fluorescein angiogram (E). This tuft of NV is connected to a network of dilated vessels in the deep (C), intermediate (B) and superficial (A) plexuses by a vessel. Cross-sectional angiogram (F) of the area indicated by yellow line in panel D shows this relationship.

**eTable.** Dilated Vessels in Intermediate and Deep Plexuses

	Dilated vessels in deep or intermediate plexus	Hairpin loops of dilated vessels in deep or intermediate plexus
PDR (N=23)	23 (100%)	9 (39.1%)
Severe NPDR (N=13)	13 (100%)	0 (0%)
Mild to Moderate NPDR (N=11)	8 (73%)	0 (0%)
Control (N=29)	0 (0%)	0 (0%)

NPDR: nonproliferative diabetic retinopathy. PDR: proliferative diabetic retinopathy.